HHS Public Access

Author manuscript

Cancer Gene Ther. Author manuscript; available in PMC 2011 October 01.

Published in final edited form as:

Cancer Gene Ther. 2011 April ; 18(4): 275–287. doi:10.1038/cgt.2010.78.

Retargeting Adenoviral Vectors to Improve Gene Transfer into Tumors

Richard T. Hogg, L.V.T.[1], **Philip Thorpe, Ph.D.**[2], and **Robert D. Gerard, Ph.D.**[1,*]

[1]Department of Internal Medicine University of Texas Southwestern Medical Center 6000 Harry Hines Blvd. NB10.218A Dallas, TX 75390-8573

[2]Department of Pharmacology University of Texas Southwestern Medical Center 6000 Harry Hines Blvd. NB10.218A Dallas, TX 75390-8573

Abstract

Gene targeting to tumors using adenoviral vectors holds great potential for cancer imaging and therapy, but the limited efficacy of current methods used to improve delivery to target tissues and reduce unwanted interactions remain substantial barriers to further development. Progress in characterizing the set of molecular interactions used by adenoviral vectors to infect particular tissues has aided the development of novel strategies for retargeting vectors to tumor cells. One method is chemical retargeting of adenovirus using bispecific antibodies against both viral capsid proteins and tumor-specific cell surface molecules. This approach can be combined either with competitive inhibitors designed to reduce viral tropism in undesired tissues, or with traditional therapeutics to increase the expression of surface molecules for improved tumor targeting. Ablating liver cell-specific interactions through mutation of capsid proteins or chemical means are promising strategies for reducing adenovirus-induced liver toxicity. The nature of tumor neovasculature also influences adenoviral delivery, and the use of vascular disrupting agents such as combretastatin can help elucidate these contributions. In this investigation, we evaluate a variety of these methods for retargeting adenoviral vectors to tumor cells *in vitro* and *in vivo*, and assess the contributions of specific molecular and tissue interactions that affect adenoviral transgene delivery.

Keywords

adenovirus; Bavituximab; bispecific antibody; fiber; targeting

* To whom correspondence should be addressed Tel 214-648-4997 Fax 214-648-1450 robert.gerard@utsouthwestern.edu.

Conflict of Interest Statement

Both Dr. Thorpe and Dr. Gerard hold equity interests in Peregrine Pharmaceuticals, a company that is commercially developing the anti-PS antibody bavituximab. Dr. Thorpe is also on the advisory board of the company and receives research support. Mr. Hogg declares no conflicts of interest.

Supplementary information is available at Cancer Gene Therapy website.

Introduction

Gene therapy holds great promise for a variety of diagnostic and therapeutic applications, and adenoviral technology has emerged as one of the primary approaches for the targeted delivery of genes to mammalian cells. Replication-deficient adenoviral (Ad) vectors based on serotypes 5 show excellent gene transfer efficiency, have high stability *in vivo*, can be grown to high titers, and techniques for their construction, propagation and purification are also well established.(1) Ad vectors have been used in the majority of all clinical trials evaluating gene therapy for cancer, and only rarely result in any serious complications. Results from trials using nontargeted adenovirus, however, have been generally disappointing.(2) This failure has mainly been attributed to the broad native tropism of adenoviral vectors which occurs primarily through high-affinity binding of the adenoviral fiber knob domain to its primary cellular receptor, the widely expressed coxsackie and adenovirus receptor (CAR).(3) Other interactions are also involved in native adenoviral infection, including those between the RGD ligand in the penton base and $\alpha_V\beta_3$ and $\alpha_V\beta_5$ integrins, interactions between the KKTK sequence in the adenoviral fiber shaft and heparin sulfate glycosaminoglycans (HSGs),(4, 5) and binding of the adenoviral hexon protein to blood coagulation factors (VII and X) which serve as a bridge for HSPG-mediated hepatocyte transduction.(6-10)

In vivo, the liver is a primary site of adenoviral infection due to hepatocyte transduction and Kuppfer cell uptake, leading to greater than 95% of hepatocytes being transduced following intravenous administration.(11) This high level of liver tropism poses numerous problems for the development of adenoviral technology as a therapeutic or imaging modality directed to other tissues, including lower viral efficacy in target tissues and virus-induced liver inflammation and toxicity.(2) A primary goal of adenoviral cancer therapy is therefore to simultaneously reduce liver transduction (detargeting) and improve the specificity of transgene expression in target tissues such as tumors and their surrounding microenvironment (targeting). Previous studies indicate that CAR and integrin-mediated interactions are unlikely to be the primary mechanisms of liver infection, since adenoviral vectors with modifications designed to ablate CAR and integrin-mediated binding have shown high residual levels of liver transduction *in vivo*.(12) Recent data, however, indicate that changing the HSG-binding site in the fiber shaft can enhance cancer cell infectivity while reducing liver transduction.(13) A more effective strategy might involve blocking the coagulation factor-hexon interactions using anticoagulant therapy such as warfarin or nematode anticoagulant protein c2 (NapC2), (7, 14-16) or through mutation of the adenoviral hexon hypervariable regions.(8, 16, 17)

Numerous approaches have been evaluated for detargeting and targeting adenoviral vectors. Ad vectors are typically detargeted using genetic modification of one or more of the three capsid proteins, hexon, penton and fiber, although chemical methods for transductional control incorporating bispecific adaptor molecules have also been used to effectively detarget adenovirus from their native tropism and retarget the virus to specific tissues. Bispecific fusion proteins or antibodies containing a high affinity knob-binding component that ablates CAR binding are attached either covalently or through a chemical linker to another component with high specificity for a surface molecule on the target cell. Successful

retargeting of vectors has been achieved using anti-knob antibodies or truncated CAR constructs chemically or genetically linked either to a variety of targeted ligands or antibodies against cell surface receptors.(12, 18-25) Results from studies using adaptor molecules have shown a 10-20 fold increase in transgene expression in target tissues *in vivo*. (24) Studies have also established correlations between augmented gene transfer and cell surface receptor density, and demonstrated a substantial reduction of reporter gene expression in the liver compared to untargeted vector.(12, 23) Preliminary evidence also indicates high stability and good *in vivo* performance for complexes involving adenoviral particles and adaptor molecules.(18, 22, 26, 27) These early results are promising, but additional studies need to be performed to achieve optimal retargeting of adenoviral vectors for cancer therapy or imaging.

Angiogenesis is an important process in the progression of solid tumors. The relatively disorganized tumor neovasculature might provide increased adenoviral access in the tumor microenvironment,(28, 29) and the utility of this effect could also be enhanced by the addition of genetic and/or physical detargeting/retargeting approaches. Tumor-specific endothelial markers of angiogenesis (TEMs) have been extensively characterized, and are rapidly being incorporated into targeted therapy strategies. Phosphatidylserine (PS) and other negatively charged phospholipids are usually restricted to the cytosolic side of cell membranes in most cells.(30-33) However, anionic phospholipids become exposed on both tumor cells and tumor vascular endothelium, but not on normal vascular endothelium in mice, making PS one of the most specific tumor markers discovered to date.(30, 31) Bavituximab is a chimeric antibody that targets exposed PS by stabilizing a complex of two β2-glycoprotein I (β2GP1) molecules that are attached to PS at the cell surface.(30, 31, 34, 35) Mouse versions of this antibody (3G4 and 2aG4) have been shown to inhibit tumor growth in multiple animal models, and a recent study shows that clear images of subcutaneous prostate tumors can be obtained in rats following tail vein injection of isotopically-labeled bavituximab.(36) Preliminary evidence indicates that antibodies against PS are rational candidates for incorporation into bispecific adaptor molecules designed to retarget adenoviral vectors to tumor tissue. The anti-microtubule chemotherapeutic docetaxel also induces the externalization of PS on several cell types, and has been shown to significantly improve antitumor activity in mice when combined with 3G4 in MDA-MB-435 tumor models.(34) The use of docetaxel in combination with PS-retargeted vectors could theoretically improve the delivery of adenoviral vectors for imaging or therapeutic purposes.

Vascular disrupting agents (VDAs) are a relatively new group of compounds that show selective disruption of tumor vasculature, primarily through the depolymerization of microtubules in the endothelial cytoskeleton.(37) Several VDAs such as combretastatin are currently in clinical development, and early results show that these agents have great potential for normalizing neovasculature, thereby reducing blood flow specifically in tumors. Although the exact mechanism of this specificity has not been firmly established, the predominant theory is that the immature and fragile nature of tumor vasculature makes it particularly susceptible to this type of therapy.(38) However, these strategies can also have undesirable effects, by potentially selecting for more malignant cells, inducing cellular adaptations that promote tumor invasion, or restricting the access of therapeutic agents to the

tumor.(39) The clinical use of antiangiogenics and VDAs therefore needs to be carefully considered in the context of other therapeutic decisions, and many researchers have suggested that the timing of antiangiogenic therapy with other agents could be an important consideration.(40) Characteristics of tumor vasculature could also affect adenoviral gene delivery for therapy or imaging purposes. Previous results in our lab have suggested that the disorganized and leaky nature of tumor blood vessels might improve adenoviral access to tumors in mice ,(28) so VDAs could be valuable for resolving the contributions of irregular tumor vasculature on adenoviral transduction efficiency.

In the present study, we sought to explore strategies for the detargeting and retargeting of adenoviral vectors to develop a platform of tumor imaging agents using luciferase as an optical reporter. Various approaches for transductional retargeting with or without the administration of ancillary agents were evaluated to improve the tumor specificity of adenoviral-mediated luciferase delivery and expression *in vitro* and *in vivo*.

Materials and Methods

Adenoviral expression vectors

AdCMVluc, with sequences from the human CMV immediate early promoter has been previously published.(41)

For construction of the luciferase vector containing mutations in the CAR and HSG binding sites (AdCMVLucHSG$^-$ CAR$^-$), the QuickChange® mutagenesis protocol (Stratagene, La Jolla, CA) was used to modify residues in the fiber knob previously shown to be involved in native CAR and HSG interactions.(42-44) Mutations K420A,K417G in fiber knob domain were used to ablate native CAR interactions, and ^{91}KKTK^{94} at the end of the third repeat in the fiber shaft was mutated to ^{91}EAGA^{94} to reduce HSG-mediated interactions. These mutations were incorporated into the recombinant viral genome cloned into pTG3602CMVlux (pTG3602 containing a CMV luciferase transgene inserted into E1) using homologous recombination in *E. coli* BJ5183.(45) The entire fiber gene was then sequenced to verify the mutations. Virus was reconstructed from the plasmid by excising the viral genome with PacI and transfection into 911 cells using Lipofectamine 2000 (Invitrogen, Carlsbad, CA).

Construction of the NapC2 expressing adenoviral vector (AdNapC2) was performed by fusing cDNA fragments encoding the secretory signal peptide from human tissue plasminogen activator (tPA) with the mature protein coding region of NapC2 under the control of the CMV promoter,(46) followed by standard homologous recombination(1) for incorporating this expression cassette into the viral genome.

All viruses were propagated and purified as previously described.(1) Briefly, large scale preparations were grown on 911 cells, harvested and purified sequentially on CsCl step gradients and Sepharose CL-4B columns equilibrated with Tris-buffered isotonic saline (137 mM NaCl, 5 mM KCl, 10 mM Tris-HCl pH7.4, 1 mM $MgCl_2$). Virus concentration was determined by optical density, with 1.0 A_{260} equal to 1×10^{12} particles/ml. Viruses were

stored frozen at -80°C after the addition of 10% glycerol at concentrations between 10^{12} and 10^{13} particles/ml until use.

Production of Soluble Fiber Knob

Soluble fiber knob was expressed in *E.coli* as a 6 histidine N-terminal tagged protein using the commercially available plasmid expression vector pQE30 from Qiagen, Inc. Expression and purification of the knob protein to homogeneity in mg quantities was carried out in a straightforward manner using IPTG induction, salt/detergent extraction of the soluble knob and affinity purification on a Ni-agarose column according to the supplier's protocols. Purified protein was dialyzed versus Tris-buffered isotonic saline containing 10% glycerol and stored frozen at -80°C.

Cell culture

Clonal HT1080 fibrosarcoma cells and MDA-MB-435 melanoma cells (originally thought to be a breast cancer line) were propagated in Dulbecco's minimal essential medium (DMEM) containing 10% fetal bovine serum (FBS). Infections of cells *in vitro* were performed with purified stocks of viruses diluted into DMEM containing 2% FBS using equivalent titers in particles per ml for infection. Cell cultures were infected for 1 hr at 37°C, and incubated overnight before cells were harvested and luciferase activity determined to assess transduction efficiency.

Construction of the bispecific antibody

Monoclonal antibodies 7H11 directed against the Ad5 fiber knob(25) and bavituximab directed against the PS:β2GP1 complex(26) were used to construct the bispecific antibody. The bispecific $F(ab')_2$ antibody derivative (bsAb) with dual specificity against the adenoviral fiber knob and phosphatidylserine (PS) was constructed by generating a natural cysteine disulfide linkage between two Fab' fragments, using their hinge region SH groups as previously described.(47) The control antibody for the bispecific detargeting/retargeting experiments consisted of a chimeric antibody of bavituximab partnered with the non-neutralizing anti- fiber knob monoclonal 2A12. Antibody purity was confirmed by SDS-PAGE followed by visualization with Coomassie Brilliant Blue, and concentration was determined by A_{280}. The dual specificity of F(ab')2 heterodimers was then confirmed by demonstrating the ability of the product to bind to both target antigens in ELISAs and cell-binding assays, as previously described.(48)

Animal experiments

All animal experiments were approved by the Institutional Animal Care and Use Committee. Female mice were used preferentially for HT1080 tumor cell implantation, although not exclusively. Mice were injected subcutaneously with $3\text{-}5\times10^6$ cells suspended in 0.5ml DMEM on the dorsal flank. Tumors were allowed to grow until 0.4-0.8 cc in size as measured by calipers, at which time either purified adenovirus or adenovirus preincubated with either the bispecific or control antibody at a fiber:bsAb ratio of 1:1 was injected via the tail vein at doses of 10^{10} or 10^{11} particles per mouse.

To determine the effect of docetaxel administration, 0.2ml of 10 mg/ml docetaxel was administered intraperitoneally 48 hr prior to virus injection. For determination of the effects of fiber knob preinjection on gene transfer efficiency, 10-20 μg of soluble fiber knob were preinjected via the tail vein 5-10 min prior to injection of adenovirus or Ad:bsAb complex. To assess the effect of combretastatin 1-phosphate (CA1P, Oxigene, Waltham, MA) on luciferase gene transfer and expression, 25 mg/Kg body weight of CA1P dissolved in normal saline was injected intraperitoneally either 6 hours before or 48 hours following injection of adenovirus.

Luciferase Imaging and Biochemical Determination

Three days after injection of adenovirus or Ad:bsAb complex, mice to be imaged were anaesthetized with isoflurane and injected subcutaneously with luciferin (0.1 mg/g body weight). Whole body luciferase activity was imaged with a Lumina bioluminescence imaging system (Caliper Biosciences, Hopkinton, MA). Total tumor light flux was quantified using the imaging software. Mice were subsequently sacrificed and major organs and tumors removed for biochemical determination of luciferase activity performed as previously described.(28) Viral DNA content in tissues was measured by real time PCR detection of the adenovirus type 5 hexon gene as previously described.(28)

Statistical Analyses

SigmaStat for Windows v3.11 was used to perform Mann-Whitney Rank Sum Test analyses for pairwise comparisons between individual treatment groups and controls.

Results

Effect of soluble fiber knob pre-injection on adenoviral gene transfer and expression in tumor bearing mice

Soluble fiber knob protein is an effective competitor for adenovirus binding to cell surface CAR. To evaluate the relative effects of knob pre-injection on adenoviral transduction and transgene expression in various tissues *in vivo*, 10^{10} particles of AdCMVLuc was administered via tail vein injection to HT1080 tumor-bearing mice either with or without pre-injection of a saturating quantity of a soluble fiber knob construct.(49, 50) Previous estimates of the initial binding capacity of a similar knob construct in a typical mouse liver was approximately 3.1 μg.(50) Based on this work, we used a 3-6 fold excess of this amount per mouse to achieve saturation. Animals were sacrificed after three days and both luciferase gene delivery and expression were assessed using biochemical methods. Results show that mean luciferase expression in both the liver and tumor (expressed as RLU per mg of wet tissue) was unaffected by fiber knob pre-injection (Figure 1, panel A). However, the tumor/liver ratio of luciferase expression was slightly lower (nearly 2-fold) when fiber knob was pre-injected ($p=0.018$), consistent with a minor effect of blocking CAR-mediated virus uptake in either tissue. A small reduction in gene delivery as assessed by viral DNA content per mg of tissue was observed in tumors of mice pre-injected with fiber knob compared to controls ($p=0.043$; Figure 1, panel B), and the expression of luciferase per viral DNA copy was also slightly reduced in tumor tissue of mice receiving fiber knob preinjection ($p=0.028$; data not shown).

Effects of detargeting adenoviral vectors by mutation of the CAR and HSG binding sites

Previous results have demonstrated significant effects of individual fiber mutations on gene transfer and expression in multiple tissues of normal mice.(43, 51) Mutations in both the HSG and CAR binding sites of the adenoviral fiber shaft and fiber knob, respectively, were therefore made to assess the contribution of HSG and CAR-mediated interactions on adenoviral infection in tumor-bearing mice. HT1080 tumor bearing mice received tail vein injections of 10^{10} or 10^{11} particles of wild-type AdCMVluc or mutant AdCMVluxHSG$^-$CAR$^-$, and luciferase gene delivery and expression were assessed in various tissues using biochemical methods. Significant reductions in luciferase expression were observed for AdCMVluxHSG$^-$CAR$^-$ compared to AdCMVluc in both liver ($p=0.03$) and tumor ($p=0.003$), an effect that was more pronounced in both tissues ($p<0.001$) using 10^{11} viral particles (Figure 1, panel C). Significant differences in tumor to liver ratios were not seen, which was expected due to overall reductions in luciferase expression in all tissues for the mutated virus compared to the wild type. Indeed, infection of HT1080 tumor cells *in vitro* by the two viruses showed that the mutant virus required a 30-fold higher concentration of viral particles to achieve luciferase expression equivalent to that of the wild type virus (data not shown). Although significant differences in adenoviral gene delivery were not observed at the 10^{10} viral dose, a significant reduction in viral DNA copy/mg of tissue was observed in the liver ($p=0.004$) and a significant increase in the tumor/liver ratio was also noted using the HSG$^-$CAR$^-$ vector compared to AdCMVLuc at the 10^{11} dose ($p=0.027$; Supplemental Figure 1, panel A). Significant reductions in luciferase expression per viral DNA copy were also observed for mutated virus compared to AdCMVluc in liver and tumor at the 10^{10} viral particle dose ($p=0.017$ and $p=0.002$, respectively), and in tumor at the 10^{11} dose ($p=0.002$; Supplemental Figure 1, panel B). These effects are most likely due to reduced liver inflammation using the detargeted virus.

Reducing liver tropism and improving tumor specificity of adenovirus using NapC2

Various reports indicate that liver tropism is largely due to interaction of the adenovirus type 5 hexon protein with serum coagulation factors.(6-10) As this mode of liver uptake can be reduced by the nematode anti-coagulant protein NapC2,(7) we tested the ability of recombinant NapC2 to block liver gene transfer and expression in mice. An adenoviral vector incorporating the CMV promoter was used to systemically express the NapC2 protein with a signal peptide from tPA to direct protein secretion from infected cells into the circulation. Varying doses of AdNapC2 were first injected into mice and after two days, the ability of 10^{11} particles of AdCMVluc to transduce liver was assayed. Results show substantially reduced AdCMVLuc gene expression in the liver at AdNapC2 doses above 10^9 particles (Figure 2, panel A). Similar reductions in gene delivery (viral DNA/mg tissue) were also observed in the liver at higher doses of AdNapC2 (Figure 2, panel B). Together these data suggest that the systemic anticoagulant NapC2 effectively reduced liver tropism and transgene expression.

An alternative approach for delivering NapC2 is to use serum from mice pre-injected with AdNapC2 as a source of the anti-coagulant factor. HT1080 tumor-bearing mice were pre-injected with 100 μl of serum collected from mice that had previously received 3×10^{10} particles of AdNapC2. Following serum injection, these mice received 10^{11} particles of

AdCMVLuc and luciferase expression was assessed after 3 days. Results showed significant reductions in luciferase expression for all tissues tested in mice that received pre-injections of NapC2 serum compared to those receiving 10^{11} particles of AdCMVLuc alone (Figure 2, panel C). This effect was most pronounced in the liver, however, which showed an 1800-fold reduction in mean luciferase expression when NapC2 serum was pre-injected ($p<0.001$ by pairwise comparison to AdCMVLuc alone). The lung had the next greatest reduction in mean luciferase expression by NapC2 serum compared to AdCMVLuc alone (160-fold; $p<0.001$ by pairwise comparison), and the mean luciferase expression in tumor was reduced 65-fold ($p=0.002$). As a result, the tumor specificity of luciferase expression per mg of tissue indicated by the tumor/liver ratio was significantly increased 6-fold in mice receiving NapC2 serum pre-injection as compared to mice receiving AdCMVLuc alone ($p=0.018$).

There were also significant reductions in gene delivery (viral DNA copy/mg tissue) for all tissues tested in mice receiving pre-injections of NapC2 serum compared to mice receiving AdCMVluc alone (data not shown), suggesting that the overall reduction in luciferase expression is a result of lower transduction efficiency due to NapC2 interference. Significant reductions in luciferase expression per viral DNA copy in tumor ($p=0.032$) and liver ($p=0.009$) were also observed, which could also help explain the lower luciferase expression due to a decreased inflammatory response in these tissues (data not shown). Overall levels of luciferase expression and gene delivery in mice pre-injected with NapC2 serum and subsequently with 10^{11} particles AdCMVLuc were quantitatively similar to those observed in mice receiving a dose of 10^{10} particles AdCMVLuc in all tissues tested, which indicates an overall effective decrease of one log infectivity for the adenoviral vector as a result of NapC2 pre-injection.

Mice with HT1080 tumors were also pre-injected with 3×10^{9} particles of AdNapC2 to permit systemic expression of the anti-coagulant protein, then injected with 10^{11} particles of AdCMVluc two days later to compare the ability of endogenously produced NapC2 to the NapC2 serum in reducing liver infectivity. Luciferase expression per mg of tissue was similar in these mice compared to those receiving NapC2 serum, with no significant differences observed in any tissue by pairwise analysis (data not shown), with the exception that there was a 35-fold increase in luciferase expression per mg of liver in mice receiving AdNapC2 compared to those that received NapC2 serum ($p=0.029$). This is probably a result of increased liver inflammation resulting from the higher viral dose when two viruses were administered. However, in all other tissues, both methods of anti-coagulation (endogenous and exogenous) appear to have similar effects on the expression of an adenovirally-delivered transgene.

Retargeting adenoviral vectors using a bispecific antibody directed to negatively charged phospholipids

Transductional targeting of adenoviral vectors is an attractive strategy to reduce liver infection and achieve greater tumor specificity for transgene delivery, and phosphatidylserine (PS) is a potentially useful target based on high levels of PS exposure on both tumor cells and tumor vasculature.(30, 31) We therefore evaluated the efficacy of a bispecific antibody capable of retargeting AdCMVluc to tumor cells. First, various amounts

of bsAb were mixed with purified adenoviral particles to obtain different ratios of bsAb to Ad fiber. Equivalent numbers of bsAb targeted viral particles were then used to infect HT1080 and MDA-MB-435S tumor cells *in* vitro, which provided an estimate of the optimal ratio for further *in vivo* experiments.

The addition of soluble fiber knob to cells prior to virus infection was used to block fiber binding to CAR, and soluble knob blocked >90% of wild type virus infectivity on HT1080 cells (Figure 3, panel A). The addition of bsAb increased adenoviral infectivity of HT1080 cells about 7-fold, which was unaffected by the addition of soluble knob. This indicates the ability of bsAb to effectively retarget virus by a mechanism that is independent of knob:CAR interactions. Lower bsAb:fiber ratios were clearly more effective at retargeting adenovirus, and excess bsAb apparently reduced overall infectivity.

Knob had no effect on wild type virus binding to MDA-MB-435S cells, suggesting that wild type virus entry into these cells is largely CAR-independent. This was expected based on previous studies showing a lack of CAR expression and a primarily integrin-mediated mechanism of adenoviral entry in MDA-MB-435S cells.(52, 53) There was a greater increase in MDA-MB-435s cell transduction (180-fold) by bsAb retargeted virus in comparison to HT1080 cells, and again, soluble knob protein had no effect on bsAb-retargeted virus infectivity. This can in part be attributed to a lack of CAR-dependent transduction of the breast cancer cells by wild type virus. Again, lower bsAb:fiber ratios were clearly more effective at retargeting adenovirus, and excess bsAb apparently reduced overall infectivity even more in MDA-MB-435s cells than HT1080 cells. Therefore, a 1:1 bsAb:fiber ratio was used for preparing Ad:bsAb complexes in all subsequent *in vivo* experiments.

The efficacy of bsAb-mediated retargeting of adenoviral vectors was next assessed in HT1080 tumor-bearing mice by administering Ad:bsAb compared to AdCMVluc via tail vein injection. Mice were sacrificed after three days and both luciferase gene expression and delivery were assessed in various tissues using biochemical methods. Results show significant decreases in luciferase expression in the heart ($p<0.001$) and spleen ($p=0.026$) for Ad:bsAb compared to AdCMVluc alone (Figure 3, panel B), which suggests bsAb-mediated detargeting of virus from these tissues. There was also a significant increase in viral targeting to the tumor with the addition of Ad:bsAb compared to AdCMVluc ($p=0.01$), but this increase was less than 2-fold and there was no significant change in tumor/liver ratio. Viral copy number per wet weight of tissue was also decreased for Ad:bsAb compared to AdCMVluc for lung ($p=0.006$) and spleen ($p=0.003$), although there was no change in heart, kidney, liver, tumor or tumor/liver ratio (Figure 3, panel C). There were also small increases in mean specific activity of expression (RLU/viral DNA copy) in lung (11-fold, $p<0.001$), liver (2.5-fold, $p=0.028$), and tumor (4.5-fold, $p=0.006$), and a small decrease in heart (3.8-fold, $p=0.038$) for Ad:bsAb compared to AdCMVluc (data not shown).

Effect of soluble fiber knob pre-injection on bsAb retargeting of adenoviral vectors in vivo

To investigate specific adenoviral molecular interactions in the context of bsAb-retargeted virus, we next evaluated the effects of pre-injected saturating amounts of soluble fiber knob on the infectivity of bsAb-AdCMVluc in the liver compared to tumor *in vivo*. Both mean

luciferase expression (Supplemental Figure 2, panel A) and gene copy number per mg of tissue (Supplemental Figure 2, panel B) was increased 3-4 fold in the tumor by pre-injection of soluble fiber knob compared to controls (p=0.003 for both by pairwise rank-sum comparison). There were no significant differences found in luciferase expression or gene delivery in liver or tumor/liver ratio due to pre-injection of fiber knob.

Docetaxel improves bsAb retargeting of adenoviral vectors in tumor bearing mice

The antimicrotubule agent docetaxel has previously been shown to induce the externalization of PS on several cell types, in addition to improving the antitumor activity of an anti-PS antibody in a murine tumor model.(34) We therefore evaluated the ability of docetaxel to improve bsAb retargeting of AdCMVluc to tumors *in vivo*. Because the antitumor activity of docetaxel alone complicates interpretation of *in vivo* data, all mice received systemic treatment with docetaxel two days prior to intravenous delivery of 10^{10} particles of AdCMVluc complexed with either the bsAb or a control antibody. Mice were sacrificed after three days and both luciferase gene delivery and expression were assessed using both bioluminescent imaging and biochemical methods.

In vivo imaging of luciferase activity showed an increase in tumor expression in Ad:bsAb treated mice as compared to controls (representative animals shown in Figure 3, Panel D). The mean photon flux increased nearly 10-fold from 1.3×10^{7} to 1.2×10^{8} in doectaxel treated mice given Ad:bsAb as compared to the control antibody, which was statistically significant (p=0.015). Biochemical results also indicate significantly increased luciferase expression per wet weight of tissue in the liver (4.5-fold, p=0.02), spleen (4.5-fold, p=0.003), tumor (50-fold, p=0.002), and the tumor/liver ratio (9-fold, p=0.026), whereas the heart showed a significant decrease (3-fold, p=0.02) in mice that received Ad:bsAb compared to the Ad:control antibody (Figure 3, panel E). The differences are primarily due to a dramatic reduction in gene expression in Ad:control antibody treated mice given docetaxel since the mean luciferase expression in tumors of mice treated with docetaxel were no higher than those in mice given the same Ad:bsAb without docetaxel (Figure 3, panel B).

Significant increases in viral DNA copy per mg tissue was also observed for kidney (p=0.034), liver (p=0.011), and tumor (p=0.011), and a significant decrease was observed in spleen (p=0.001) in mice receiving Ad:bsAb compared to controls (Figure 3, panel F). Changes in mean values of viral copy/mg in liver (3-4 fold) and tumor (nearly 30-fold) correlated well with increases in mean RLU/mg for these tissues, indicating that increased luciferase expression is likely due to improved transduction efficiency for the bsAb-retargeted virus compared to control virus in the context of docetaxel treatment. No significant increase in luciferase expression per viral DNA copy were observed in any tissues except for spleen (data not shown) which likely explains the increase in luciferase expression despite a reduction in DNA copy number in this tissue.

Effect of combretastatin A-1-P (CA1P) on tumor specificity following AdCMVluc administration

Combretastatin has been shown to specifically disrupt tumor vasculature.(37) Previous results in our lab also suggest that the disorganized and leaky vasculature normally present

in solid tumors can increase adenoviral access to tumor tissue.(28) We therefore evaluated the effects of CA1P treatment given either 6 hours before or 48 hours after systemic administration of 10^{10} particles of AdCMVluc. Results show a highly significant decrease in luciferase expression per mg tissue in tumor ($p<0.001$) and a highly significant increase in the liver ($p<0.001$) following pretreatment with CA1P (Figure 4, panel A). These changes in RLU/mg translated into a 160-fold decrease in tumor specificity shown by the tumor/liver ratio of RLU/mg values ($p<0.001$). By contrast, luciferase expression in tissues of mice given combretastatin 48 hours after receiving AdCMVluc was indistinguishable from controls. This suggests that pre-treatment effects are due to decreased tumor accessibility to virus in mice whose tumor vasculature had been normalized by CA1P pretreatment. Significant changes in viral DNA per mg of tissue were not observed in liver or tumor following CA1P pretreatment compared to controls (Figure 4, panel B), indicating that the difference in luciferase expression in liver observed for CA1P pretreatment is due to effects other than a change in transduction frequency. Indeed, luciferase expression normalized to viral DNA copy number (Figure 4, panel C) is substantially higher in the liver ($p<0.001$) following CA1P pretreatment compared to controls, whereas expression per DNA copy was lower in the tumor ($p<0.001$). Increased CMV-driven expression in the liver in addition to decreased tumor expression following CA1P treatment are the primary factors resulting in decreased tumor specificity following CA1P pretreatment.

The effects of CA1P are readily visualized by correlating the total tumor photon flux quantified by bioluminescent imaging (Figure 4, panel D) with the biochemically determined luciferase activity. Similar decreases in both total photon flux and luciferase activity determined biochemically are seen in the tumor following pretreatment with CA1P as compared to controls receiving no CA1P (Figure 4, panel E). In mice receiving CA1P 48 hours after administration of virus, however, only tumor photon flux is decreased as compared to control mice. This differential effect is likely due to the decreased tumor availability of the luciferin given to mice immediately prior to bioluminescent imaging, whereas biochemically determined luciferase expression is unaffected because the full complement of virus has been delivered prior to CA1P-mediated disruption of the tumor vasculature.

Discussion

Adenoviral technology remains a promising method to deliver transgenes to tumor cells for imaging or therapeutic purposes, but a number of complicating factors still need to be addressed. A central issue is the broad native tropism of systemically administered adenovirus, including the high levels of liver infectivity widely observed for unmodified virus.(11) This represents a substantial problem for the clinical development of adenoviral vectors, because high liver infectivity could result in hepatic toxicity and also reduces the amount of adenovirus available for infecting tumor cells. To investigate various methods for reducing liver infection, we first assessed the ability of soluble fiber knob to compete for adenovirus binding to CAR and alter the tropism of wild-type adenovirus. Preinjection of knob protein, however, had little effect on the infectivity of wild-type virus in the liver or tumor in our investigation. Other interactions such as those between HSGs and the adenoviral shaft have also been shown to be important for liver infection.(13) To evaluate

the effects of ablating multiple adenoviral interactions, we also evaluated an adenoviral construct with dual mutations in the CAR and HSG-binding sites located in the fiber knob and fiber shaft, respectively. Although HSG-CAR-modified virus resulted in significantly lower luciferase expression compared to wild-type, similar reductions were also seen in all other tissues including tumor. Our results therefore suggest that the elimination of both CAR and HSG interactions is unlikely to improve the tumor specificity of adenoviral infection.

Because of previous work by others suggesting the crucial importance of FX-mediated interactions for adenoviral liver infectivity, we also evaluated the ability of a FX-binding anticoagulant protein (NapC2) for reducing liver transduction and improving the tumor specificity of adenoviral infection. Preliminary data in non-tumor bearing animals indicated that NapC2 expression effectively reduced subsequent adenoviral infection in the liver, but data in tumor-bearing animals showed a global reduction of Ad infectivity across all tissues tested. This effect was most pronounced in the liver, in agreement with previous studies showing the greater importance of FX-mediated interactions in adenoviral tropism to hepatocytes.(6, 7, 10, 15, 16, 54). Consistent with our results, these data also suggest that FX-mediated interactions are important for adenoviral infection in epithelial cells, spleen and lung, in addition to several types of tumor cells.(6-8, 14-16, 55) To our knowledge, ours is the most extensive *in vivo* analysis of the effects of NapC2 on subsequent adenoviral infection in a variety of tissues. Our data, when combined with previous studies, suggests that adenoviral vectors might use FX-mediated interactions for infecting more types of cells and tissues than previously believed. Thus, strategies designed to ablate FX-dependent adenoviral infection of the liver need to be combined with additional retargeting strategies to improve the overall therapeutic index of these approaches.

Chemical retargeting of adenoviral vectors using bispecific adaptor molecules is an attractive option to reduce undesired native interactions and improve the tumor specificity of adenoviral transgene delivery. We evaluated a bispecific antibody (bsAb) directed against adenoviral fiber knob and PS for its ability to retarget wild-type adenovirus to tumor tissue *in vivo*, based on the tendency of tumor endothelium to externalize PS compared to normal tissue.(30, 31) The small but significant increase in luciferase expression we observed using bsAb compared to wild-type virus alone *in vivo* was largely expected based on *in vitro* results. Interestingly, gene delivery assessed by viral DNA copy per mg of tissue was lower in all tissues including tumor with the addition of bsAb compared to controls. In fact, improved transcription with the addition of bsAb rather than increased transduction appeared to be the primary reason for the increase in tumor luciferase expression. This was unexpected based on the physical retargeting method, which should have led to improved tumor specificity exclusively by increasing the frequency of viral gene delivery in tumor tissue. The addition of soluble fiber knob prior to systemic administration of bsAb-retargeted virus, however, improved both luciferase expression and gene delivery in tumor tissue, suggesting that reducing viral interactions with non-target tissues may increase the amount of bsAb-retargeted virus available for tumor cell infection. Experiments performed on the background of docetaxel treatment showed an even greater improvement in mean transgene expression in the tumor and a significant improvement in tumor specificity for bsAb retargeted virus. In addition, docetaxel resulted in a significant increase in viral gene

delivery in the tumor, suggesting that doectaxel increased the externalization of PS and improved PS-directed adenoviral retargeting. The mean values of luciferase expression in tumor were quantitatively similar to those observed with no docetaxel treatment, however, so the ability of docetaxel to substantially increase adenoviral retargeting of tumors is difficult to interpret.

Previous results from our lab suggest that the disorganized and leaky tumor vasculature might improve adenoviral access to tumors in mice,(28) so we further investigated this possibility using the tumor-specific vascular disrupting agent CA1P. Pretreatment with CA1P clearly decreased luciferase expression in tumors, whereas treatment with CA1P two days following adenovirus administration had no effect. This indicated that disrupting tumor vasculature significantly restricts viral access to tumors, but has little effect on transgene expression following the delivery of wild-type virus to tumor cells. CA1P pretreatment had the opposite effect in the liver, showing an increase in liver transgene expression. This could indicate that virus excluded from the tumor because of vascular disruption became available to infect other tissues such as liver. The higher observed luciferase expression per viral DNA copy in the liver, however, could also be partially explained by increased hepatic inflammation driving expression from the inflammatory responsive CMV promoter. The correlation of biochemical and bioluminescent data also showed that vascular disruption apparently reduces tumor access to luciferin. Unlike adenovirus, luciferin is a small molecule substrate whose access to the tumor was substantially restricted following CA1P administration. This provides additional evidence that the timing of anti-vascular agents could be important for efficacy when combined with cytotoxic or targeted therapies, and these results overall suggest that issues related to the immediate tumor microenvironment will be important considerations during the optimization of adenoviral technology for therapeutic or imaging purposes.

Modified adenoviral vectors have great potential for the tumor-specific delivery of genes expressing therapeutic or imaging agents, but more effective methods for detargeting adenovirus from their native interactions and improving tumor specificity must be developed. Results from this investigation demonstrate that a bispecific antibody against the adenoviral fiber knob and PS can be effective for retargeting adenovirus to tumor cells, and that the co-administration of docetaxel to increase PS expression on tumor vasculature or the use of competitive inhibitors to reduce native interactions with non-target tissues improved the overall effectiveness of this approach. The use of vascular disrupting agents such as CA1P for modifying the tumor vasculature as well as the transcriptional microenvironment of the tumor to drive the expression of adenoviral delivered genes also needs further evaluation. The complex and ever-changing landscape of tumor biology suggests that adenoviral therapy will require optimization for particular tumors and physiological conditions, and results from this study support the idea that issues related to tumor microenvironment will be important for the continued development of adenoviral-based cancer therapy.

Supplementary Material

Refer to Web version on PubMed Central for supplementary material.

Acknowledgements

The authors wish to thank Julie Poirot and Jessica Mullens for technical help with recombinant virus construction and preparation, and Shuzhen Li for preparation of the bispecific antibodies and providing the purified β2GP1 protein. Paul Card helped prepare the manuscript for publication. Bavituximab was generously provided by Peregrine Pharmaceuticals Inc., Tustin, CA, and Oxigene (Waltham, MA) generously provided the combretastatin 1 phosphate. Optical imaging was facilitated by the UT Southwestern Small Animal Imaging Research Program funded by NCI U24 CA126608. This work was supported by a Texas Higher Education Coordinating Board Advanced Technology Program grant and by NIH R01 CA115935 to RDG, and by the Gillson Longenbaugh Foundation to PT.

References

1. Gerard, RD.; Meidell, RS. Adenovirus vectors. In: Hames, BD.; Glover, D., editors. DNA Cloning: A Practical Approach. Oxford University Press; Oxford: 1995. p. 285-307.
2. Glasgow JN, Everts M, Curiel DT. Transductional targeting of adenovirus vectors for gene therapy. Cancer Gene Ther. 2006; 13:830–844. [PubMed: 16439993]
3. Tomko RP, Xu R, Philipson L. HCAR and MCAR: the human and mouse cellular receptors for subgroup C adenoviruses and group B coxsackieviruses. Proc Natl Acad Sci U S A. 1997; 94:3352–3356. [PubMed: 9096397]
4. Dechecchi MC, Melotti P, Bonizzato A, Santacatterina M, Chilosi M, Cabrini G. Heparan sulfate glycosaminoglycans are receptors sufficient to mediate the initial binding of adenovirus types 2 and 5. J Virol. 2001; 75:8772–8780. [PubMed: 11507222]
5. Dechecchi MC, Tamanini A, Bonizzato A, Cabrini G. Heparan sulfate glycosaminoglycans are involved in adenovirus type 5 and 2-host cell interactions. Virology. 2000; 268:382–390. [PubMed: 10704346]
6. Kalyuzhniy O, Di Paolo NC, Silvestry M, Hofherr SE, Barry MA, Stewart PL, Shayakhmetov DM. Adenovirus serotype 5 hexon is critical for virus infection of hepatocytes in vivo. Proc Natl Acad Sci U S A. 2008; 105:5483–5488. [PubMed: 18391209]
7. Waddington SN, McVey JH, Bhella D, Parker AL, Barker K, Atoda H, Pink R, Buckley SM, Greig JA, Denby L, Custers J, Morita T, Francischetti IM, Monteiro RQ, Barouch DH, van Rooijen N, Napoli C, Havenga MJ, Nicklin SA, Baker AH. Adenovirus serotype 5 hexon mediates liver gene transfer. Cell. 2008; 132:397–409. [PubMed: 18267072]
8. Alba R, Bradshaw AC, Parker AL, Bhella D, Waddington SN, Nicklin SA, van Rooijen N, Custers J, Goudsmit J, Barouch DH, McVey JH, Baker AH. Identification of coagulation factor (F)X binding sites on the adenovirus serotype 5 hexon: effect of mutagenesis on FX interactions and gene transfer. Blood. 2009; 114:965–971. [PubMed: 19429866]
9. Kremer EJ. Mutagenesis of hexon “FX” hepatic tropism. Blood. 2009; 114:929–930. [PubMed: 19643990]
10. Vigant F, Descamps D, Jullienne B, Esselin S, Connault E, Opolon P, Tordjmann T, Vigne E, Perricaudet M, Benihoud K. Substitution of hexon hypervariable region 5 of adenovirus serotype 5 abrogates blood factor binding and limits gene transfer to liver. Mol Ther. 2008; 16:1474–1480. [PubMed: 18560416]
11. Li Q, Kay MA, Finegold M, Stratford-Perricaudet LD, Woo SL. Assessment of recombinant adenoviral vectors for hepatic gene therapy. Hum Gene Ther. 1993; 4:403–409. [PubMed: 8399487]
12. Sharma A, Li X, Bangari DS, Mittal SK. Adenovirus receptors and their implications in gene delivery. Virus Res. 2009; 143:184–194. [PubMed: 19647886]
13. Bayo-Puxan N, Gimenez-Alejandre M, Lavilla-Alonso S, Gros A, Cascallo M, Hemminki A, Alemany R. Replacement of adenovirus type 5 fiber shaft heparan sulfate proteoglycan-binding domain with RGD for improved tumor infectivity and targeting. Hum Gene Ther. 2009; 20:1214–1221. [PubMed: 19537946]
14. Gimenez-Alejandre M, Cascallo M, Bayo-Puxan N, Alemany R. Coagulation factors determine tumor transduction in vivo. Hum Gene Ther. 2008; 19:1415–1419. [PubMed: 18795826]

15. Parker AL, Waddington SN, Nicol CG, Shayakhmetov DM, Buckley SM, Denby L, Kemball-Cook G, Ni S, Lieber A, McVey JH, Nicklin SA, Baker AH. Multiple vitamin K-dependent coagulation zymogens promote adenovirus-mediated gene delivery to hepatocytes. Blood. 2006; 108:2554–2561. [PubMed: 16788098]
16. Waddington SN, Parker AL, Havenga M, Nicklin SA, Buckley SM, McVey JH, Baker AH. Targeting of adenovirus serotype 5 (Ad5) and 5/47 pseudotyped vectors in vivo: fundamental involvement of coagulation factors and redundancy of CAR binding by Ad5. J Virol. 2007; 81:9568–9571. [PubMed: 17553882]
17. Shashkova EV, Doronin K, Senac JS, Barry MA. Macrophage depletion combined with anticoagulant therapy increases therapeutic window of systemic treatment with oncolytic adenovirus. Cancer Res. 2008; 68:5896–5904. [PubMed: 18632644]
18. Dmitriev I, Kashentseva E, Rogers BE, Krasnykh V, Curiel DT. Ectodomain of coxsackievirus and adenovirus receptor genetically fused to epidermal growth factor mediates adenovirus targeting to epidermal growth factor receptor-positive cells. J Virol. 2000; 74:6875–6884. [PubMed: 10888627]
19. Douglas JT, Rogers BE, Rosenfeld ME, Michael SI, Feng M, Curiel DT. Targeted gene delivery by tropism-modified adenoviral vectors. Nat Biotechnol. 1996; 14:1574–1578. [PubMed: 9634824]
20. Goldman CK, Rogers BE, Douglas JT, Sosnowski BA, Ying W, Siegal GP, Baird A, Campain JA, Curiel DT. Targeted gene delivery to Kaposi's sarcoma cells via the fibroblast growth factor receptor. Cancer Res. 1997; 57:1447–1451. [PubMed: 9108444]
21. Gu DL, Gonzalez AM, Printz MA, Doukas J, Ying W, D'Andrea M, Hoganson DK, Curiel DT, Douglas JT, Sosnowski BA, Baird A, Aukerman SL, Pierce GF. Fibroblast growth factor 2 retargeted adenovirus has redirected cellular tropism: evidence for reduced toxicity and enhanced antitumor activity in mice. Cancer Res. 1999; 59:2608–2614. [PubMed: 10363982]
22. Kashentseva EA, Seki T, Curiel DT, Dmitriev IP. Adenovirus targeting to cerbB-2 oncoprotein by single-chain antibody fused to trimeric form of adenovirus receptor ectodomain. Cancer Res. 2002; 62:609–616. [PubMed: 11809717]
23. Li HJ, Everts M, Pereboeva L, Komarova S, Idan A, Curiel DT, Herschman HR. Adenovirus tumor targeting and hepatic untargeting by a coxsackie/adenovirus receptor ectodomain anti-carcinoembryonic antigen bispecific adapter. Cancer Res. 2007; 67:5354–5361. [PubMed: 17545616]
24. Reynolds PN, Zinn KR, Gavrilyuk VD, Balyasnikova IV, Rogers BE, Buchsbaum DJ, Wang MH, Miletich DJ, Grizzle WE, Douglas JT, Danilov SM, Curiel DT. A targetable, injectable adenoviral vector for selective gene delivery to pulmonary endothelium in vivo. Mol Ther. 2000; 2:562–578. [PubMed: 11124057]
25. Israel BF, Pickles RJ, Segal DM, Gerard RD, Kenney SC. Enhancement of adenovirus vector entry into CD70-positive B-cell Lines by using a bispecific CD70-adenovirus fiber antibody. J Virol. 2001; 75:5215–5221. [PubMed: 11333903]
26. Itoh A, Okada T, Mizuguchi H, Hayakawa T, Mizukami H, Kume A, Takatoku M, Komatsu N, Hanazono Y, Ozawa K. A soluble CAR-SCF fusion protein improves adenoviral vector-mediated gene transfer to c-Kit-positive hematopoietic cells. J Gene Med. 2003; 5:929–940. [PubMed: 14601130]
27. Kim J, Smith T, Idamakanti N, Mulgrew K, Kaloss M, Kylefjord H, Ryan PC, Kaleko M, Stevenson SC. Targeting adenoviral vectors by using the extracellular domain of the coxsackie-adenovirus receptor: improved potency via trimerization. J Virol. 2002; 76:1892–1903. [PubMed: 11799184]
28. Hogg RT, Garcia JA, Gerard RD. Adenoviral targeting of gene expression to tumors. Cancer Gene Ther. 17:375–386. [PubMed: 20139924]
29. Ocak I, Baluk P, Barrett T, McDonald DM, Choyke P. The biologic basis of in vivo angiogenesis imaging. Front Biosci. 2007; 12:3601–3616. [PubMed: 17485324]
30. Ran S, Downes A, Thorpe PE. Increased exposure of anionic phospholipids on the surface of tumor blood vessels. Cancer Res. 2002; 62:6132–6140. [PubMed: 12414638]

31. Ran S, Thorpe PE. Phosphatidylserine is a marker of tumor vasculature and a potential target for cancer imaging and therapy. Int J Radiat Oncol Biol Phys. 2002; 54:1479–1484. [PubMed: 12459374]
32. Ran S, Gao B, Duffy S, Watkins L, Rote N, Thorpe PE. Infarction of solid Hodgkin's tumors in mice by antibody-directed targeting of tissue factor to tumor vasculature. Cancer Res. 1998; 58:4646–4653. [PubMed: 9788617]
33. Ran S, He J, Huang X, Soares M, Scothorn D, Thorpe PE. Antitumor effects of a monoclonal antibody that binds anionic phospholipids on the surface of tumor blood vessels in mice. Clin Cancer Res. 2005; 11:1551–1562. [PubMed: 15746060]
34. Huang X, Bennett M, Thorpe PE. A monoclonal antibody that binds anionic phospholipids on tumor blood vessels enhances the antitumor effect of docetaxel on human breast tumors in mice. Cancer Res. 2005; 65:4408–4416. [PubMed: 15899833]
35. Luster TA, He J, Huang X, Maiti SN, Schroit AJ, de Groot PG, Thorpe PE. Plasma protein beta-2-glycoprotein 1 mediates interaction between the anti-tumor monoclonal antibody 3G4 and anionic phospholipids on endothelial cells. J Biol Chem. 2006; 281:29863–29871. [PubMed: 16905548]
36. Jennewein M, Lewis MA, Zhao D, Tsyganov E, Slavine N, He J, Watkins L, Kodibagkar VD, O'Kelly S, Kulkarni P, Antich PP, Hermanne A, Rosch F, Mason RP, Thorpe PE. Vascular imaging of solid tumors in rats with a radioactive arsenic-labeled antibody that binds exposed phosphatidylserine. Clin Cancer Res. 2008; 14:1377–1385. [PubMed: 18316558]
37. Kanthou C, Tozer GM. Microtubule depolymerizing vascular disrupting agents: novel therapeutic agents for oncology and other pathologies. Int J Exp Pathol. 2009; 90:284–294. [PubMed: 19563611]
38. Tozer GM, Kanthou C, Baguley BC. Disrupting tumour blood vessels. Nat Rev Cancer. 2005; 5:423–435. [PubMed: 15928673]
39. Michieli P. Hypoxia, angiogenesis and cancer therapy: to breathe or not to breathe? Cell Cycle. 2009; 8:3291–3296. [PubMed: 19770588]
40. Kerbel RS. Antiangiogenic therapy: a universal chemosensitization strategy for cancer? Science. 2006; 312:1171–1175. [PubMed: 16728631]
41. Herz J, Gerard RD. Adenovirus-mediated transfer of low density lipoprotein receptor gene acutely accelerates cholesterol clearance in normal mice. Proc Natl Acad Sci U S A. 1993; 90:2812–2816. [PubMed: 8464893]
42. Roelvink PW, Mi Lee G, Einfeld DA, Kovesdi I, Wickham TJ. Identification of a conserved receptor-binding site on the fiber proteins of CAR-recognizing adenoviridae. Science. 1999; 286:1568–1571. [PubMed: 10567265]
43. Smith TA, Idamakanti N, Rollence ML, Marshall-Neff J, Kim J, Mulgrew K, Nemerow GR, Kaleko M, Stevenson SC. Adenovirus serotype 5 fiber shaft influences in vivo gene transfer in mice. Hum Gene Ther. 2003; 14:777–787. [PubMed: 12804140]
44. Smith TA, Idamakanti N, Marshall-Neff J, Rollence ML, Wright P, Kaloss M, King L, Mech C, Dinges L, Iverson WO, Sherer AD, Markovits JE, Lyons RM, Kaleko M, Stevenson SC. Receptor interactions involved in adenoviral-mediated gene delivery after systemic administration in non-human primates. Hum Gene Ther. 2003; 14:1595–1604. [PubMed: 14633402]
45. Chartier C, Degryse E, Gantzer M, Dieterle A, Pavirani A, Mehtali M. Efficient generation of recombinant adenovirus vectors by homologous recombination in Escherichia coli. J Virol. 1996; 70:4805–4810. [PubMed: 8676512]
46. Kopfler WP, Willard M, Betz T, Willard JE, Gerard RD, Meidell RS. Adenovirus-mediated transfer of a gene encoding human apolipoprotein A-I into normal mice increases circulating high-density lipoprotein cholesterol. Circulation. 1994; 90:1319–1327. [PubMed: 8087941]
47. Brennan M, Davison PF, Paulus H. Preparation of bispecific antibodies by chemical recombination of monoclonal immunoglobulin G1 fragments. Science. 1985; 229:81–83. [PubMed: 3925553]
48. Huang X, Molema G, King S, Watkins L, Edgington TS, Thorpe PE. Tumor infarction in mice by antibody-directed targeting of tissue factor to tumor vasculature. Science. 1997; 275:547–550. [PubMed: 8999802]

49. Henry LJ, Xia D, Wilke ME, Deisenhofer J, Gerard RD. Characterization of the knob domain of the adenovirus type 5 fiber protein expressed in Escherichia coli. J Virol. 1994; 68:5239–5246. [PubMed: 8035520]

50. Zinn KR, Douglas JT, Smyth CA, Liu HG, Wu Q, Krasnykh VN, Mountz JD, Curiel DT, Mountz JM. Imaging and tissue biodistribution of 99mTc-labeled adenovirus knob (serotype 5). Gene Ther. 1998; 5:798–808. [PubMed: 9747460]

51. Bayo-Puxan N, Cascallo M, Gros A, Huch M, Fillat C, Alemany R. Role of the putative heparan sulfate glycosaminoglycan-binding site of the adenovirus type 5 fiber shaft on liver detargeting and knob-mediated retargeting. J Gen Virol. 2006; 87:2487–2495. [PubMed: 16894186]

52. Niu G, Xiong Z, Cheng Z, Cai W, Gambhir SS, Xing L, Chen X. In vivo bioluminescence tumor imaging of RGD peptide-modified adenoviral vector encoding firefly luciferase reporter gene. Mol Imaging Biol. 2007; 9:126–134. [PubMed: 17297551]

53. Xiong Z, Cheng Z, Zhang X, Patel M, Wu JC, Gambhir SS, Chen X. Imaging chemically modified adenovirus for targeting tumors expressing integrin alphavbeta3 in living mice with mutant herpes simplex virus type 1 thymidine kinase PET reporter gene. J Nucl Med. 2006; 47:130–139. [PubMed: 16391197]

54. Shayakhmetov DM, Gaggar A, Ni S, Li ZY, Lieber A. Adenovirus binding to blood factors results in liver cell infection and hepatotoxicity. J Virol. 2005; 79:7478–7491. [PubMed: 15919903]

55. Jonsson MI, Lenman AE, Frangsmyr L, Nyberg C, Abdullahi M, Arnberg N. Coagulation factors IX and X enhance binding and infection of adenovirus types 5 and 31 in human epithelial cells. J Virol. 2009; 83:3816–3825. [PubMed: 19158249]

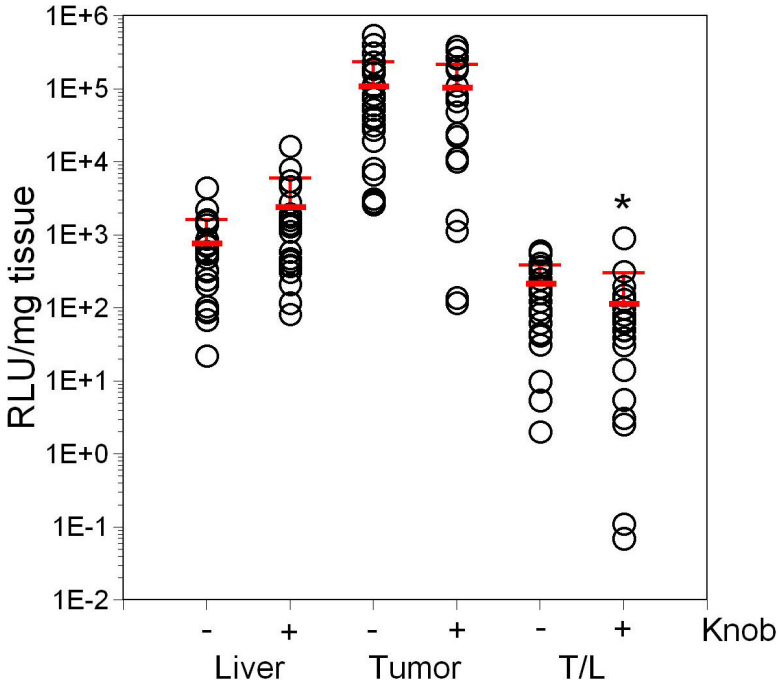

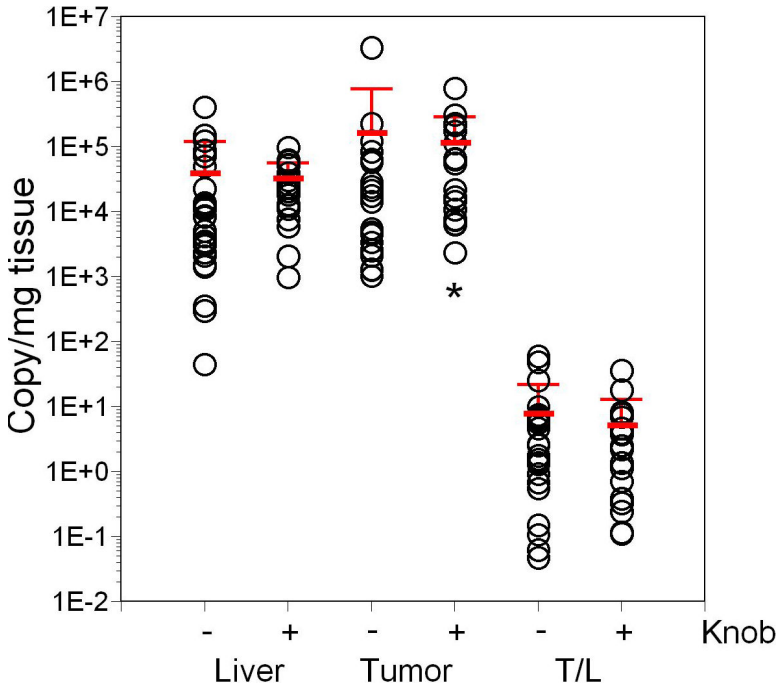

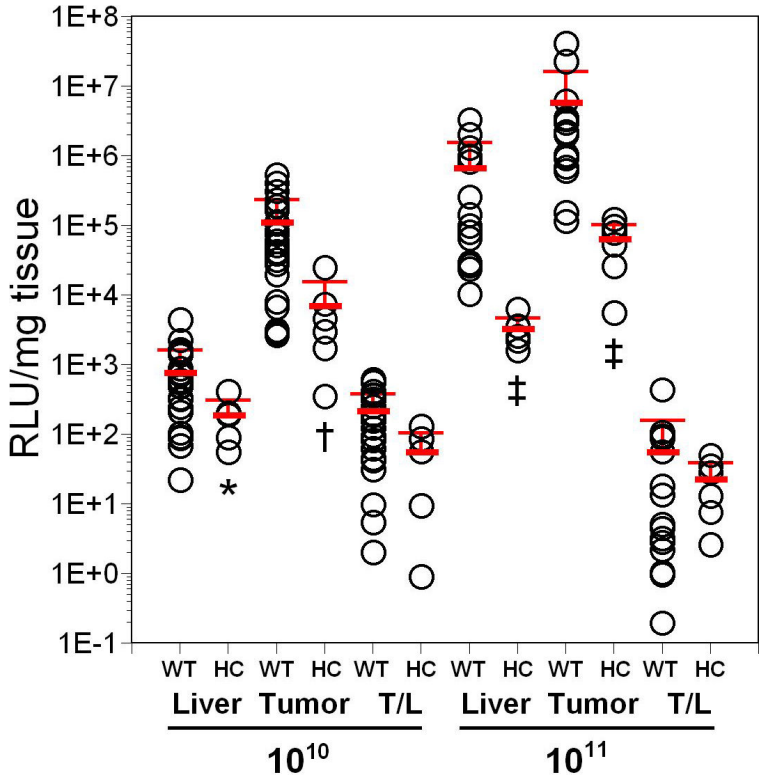

Figure 1. Effect of soluble fiber knob pre-injection and fiber detargeting mutations on adenoviral luciferase gene transfer and expression in tumor-bearing mice

Values for individual mice are shown as circles, with mean and standard deviation shown by horizontal and error bars. Significant differences between experimental and control groups are indicated by asterisks (*; $p<0.05$), daggers (†; $p\leq0.01$), and double daggers ($p\leq0.001$). Panels A and B, Effect of fiber knob preinjection on luciferase expression and gene delivery. Mice were injected with10^{10} particles AdCMVLuc either with (+) or without (-) pre-injection of a 3-6 fold excess of soluble fiber knob. Panel A, Luciferase expression was quantified in tumor and liver using biochemical means and is expressed in relative light units (RLU) per milligram of tissue. Panel B, Effect of fiber knob pre-injection on biodistribution of viral DNA. Gene delivery in viral DNA copy per mg of tissue was measured in liver and tumor using real-time PCR. Panel C, Effect of fiber detargeting mutations on luciferase expression in HT1080 tumor-bearing mice following the administration of 10^{10} or 10^{11} particles of either AdCMVLuc (WT) or the detargeted vector (HC) containing mutations in the HSG and CAR binding sites (AdCMVLucHSGCAR^{-}). Luciferase expression was quantified in tumor and liver using biochemical means and is expressed in relative light units (RLU) per milligram of tissue.

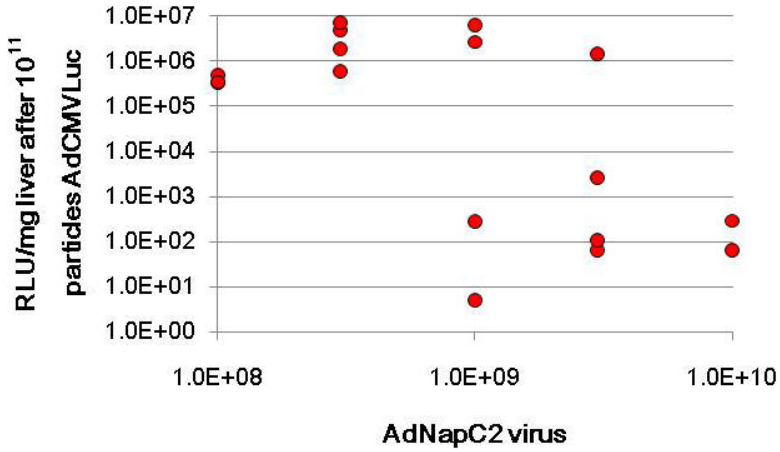

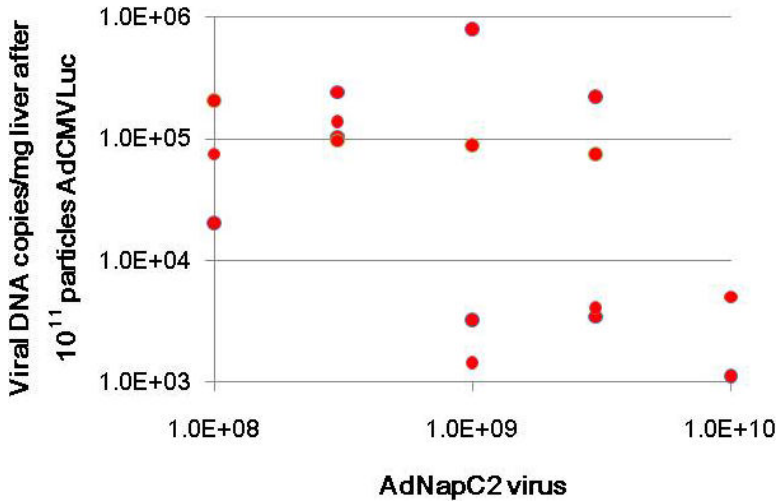

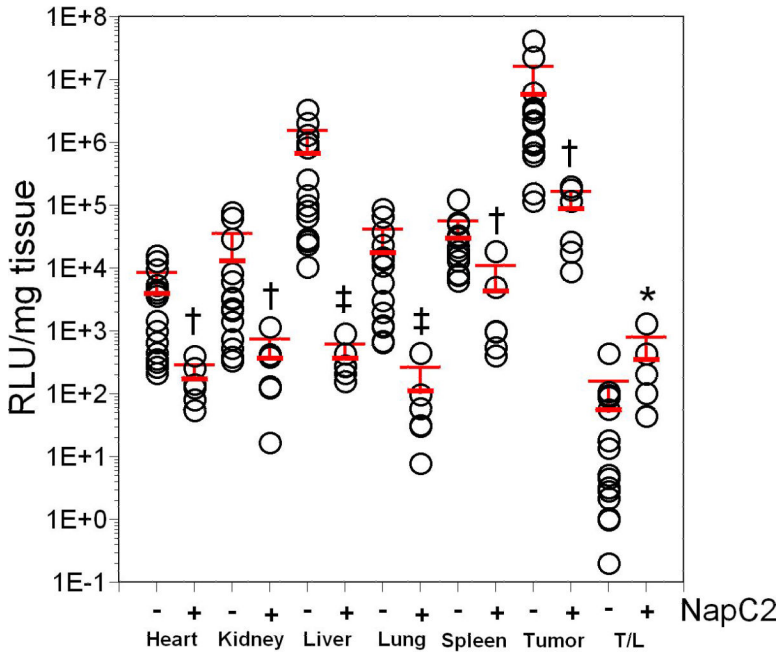

Figure 2. Effect of NapC2 anticoagulant protein on gene transfer and expression in mice

Varying doses of AdNApC2 virus were injected intravenously into mice, and two days later 10^{11} particles of AdCMVLuc were injected to assess the effect of NapC2 expression on liver gene transfer and expression. Panel A, Luciferase expression per mg of liver tissue in mice without tumors. Panel B, Viral DNA copy number per mg of liver tissue in mice without tumors. Panel C, HT1080 tumor bearing mice were pre-injected with 100μl serum from mice that had received 3×10^{10} particles of AdNapC2 two days before. Ten minutes following injection of serum, mice received 10^{11} particles AdCMVLuc. Luciferase expression in various tissues was measured after 3 days, and the tumor/liver ratio calculated. Values for individual mice are shown, and significant differences between experimental and control groups are indicated by asterisks (*; $p<0.05$), daggers (†; $p\leq0.01$), and double daggers ($p\leq0.001$). Mean and standard deviation are shown by horizontal and error bars.

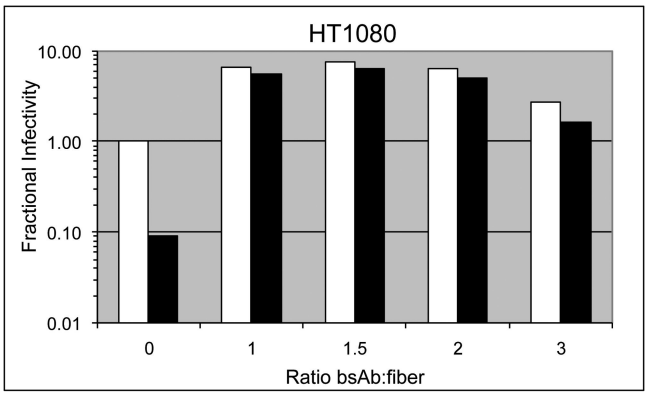

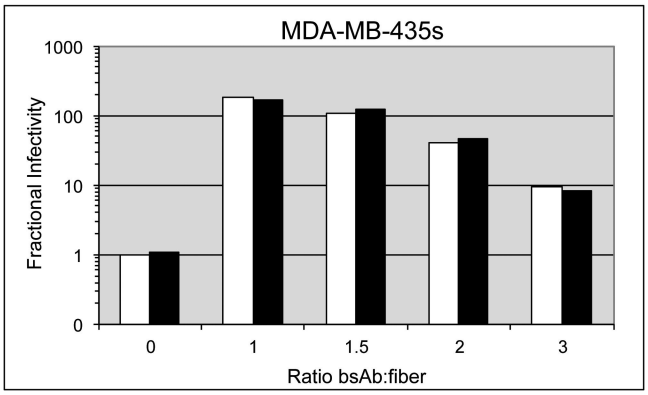

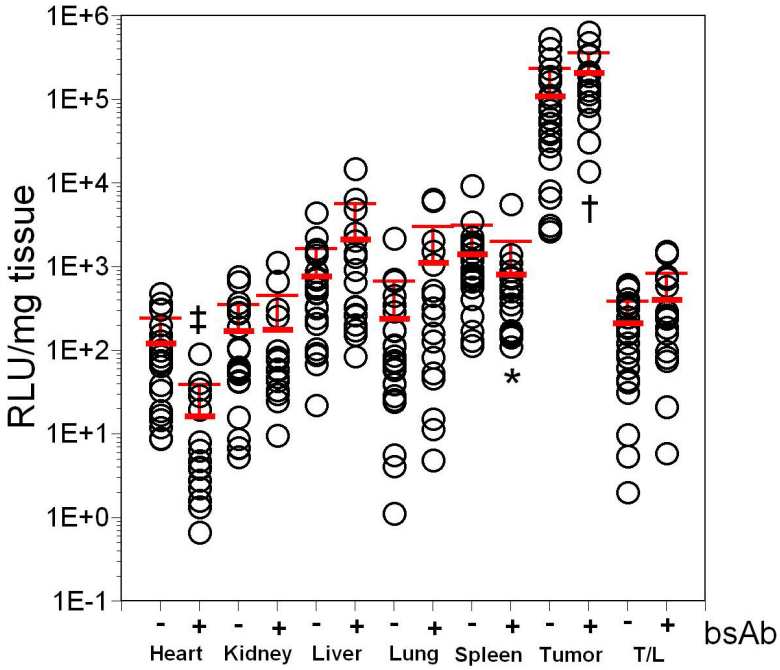

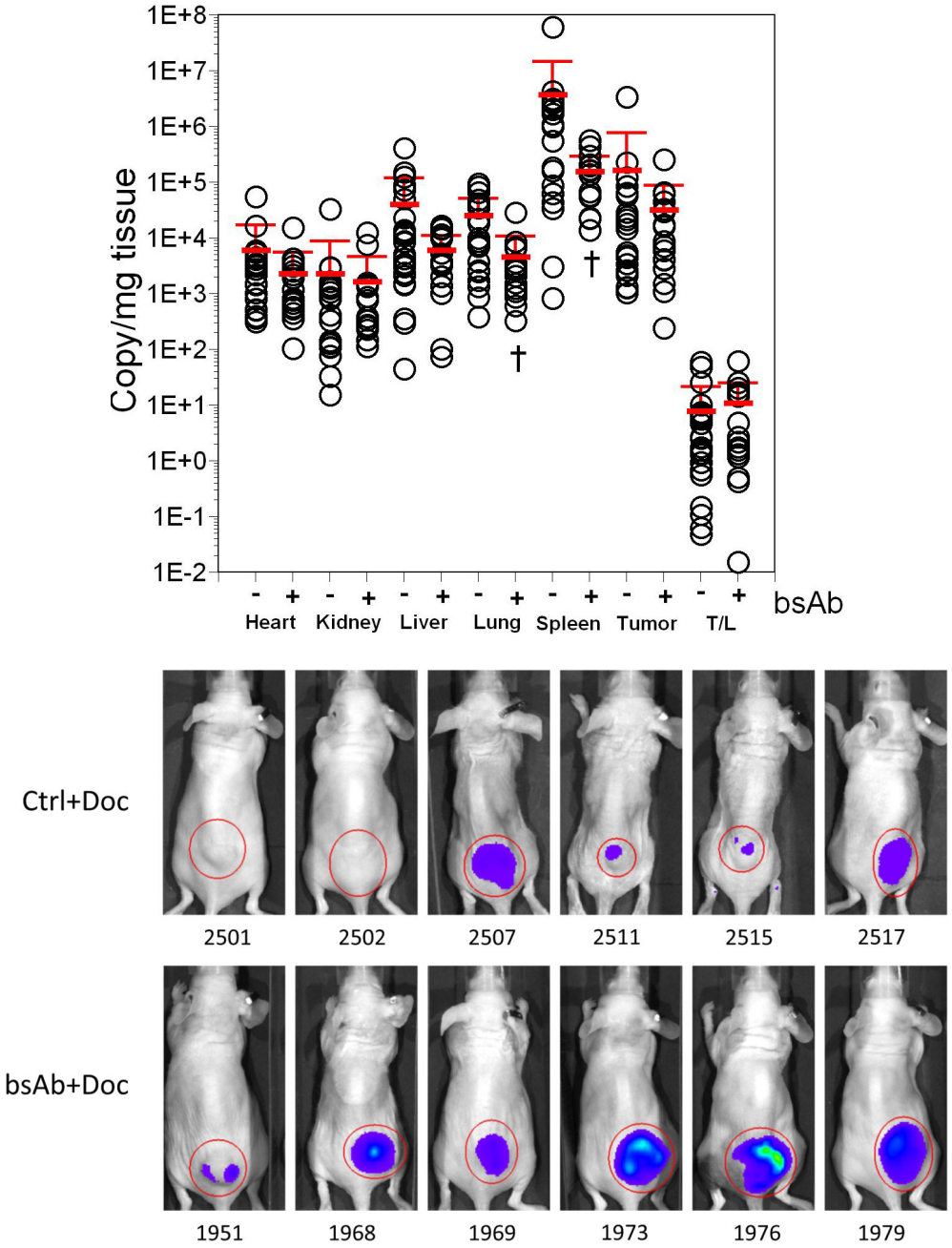

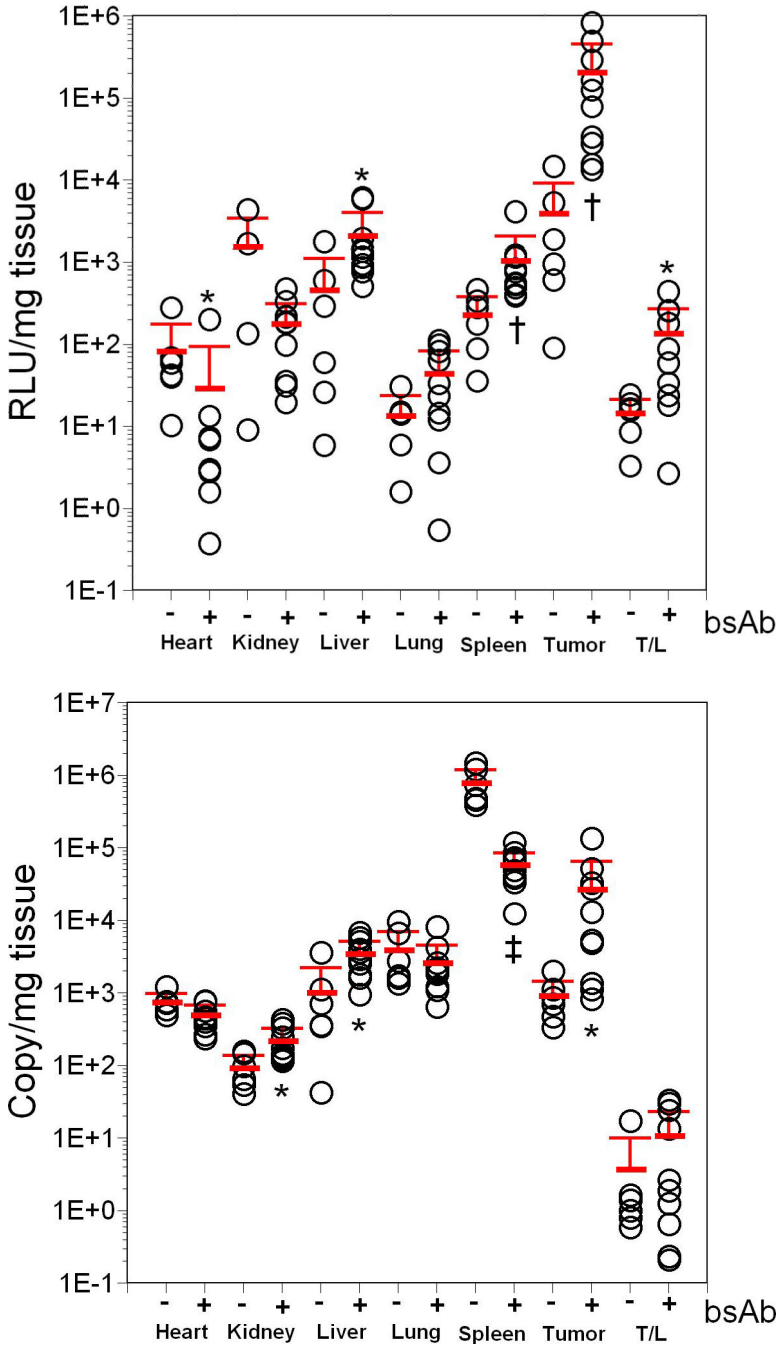

Figure 3. Effect of 7H11:bavituximab bispecific antibody (bsAb) retargeting of AdCMVLuc in vitro and in vivo

Panel A, Effect of bsAb on tumor cell infection *in vitro*. Tumor cells either expressing CAR (HT1080) or lacking CAR expression (MDA-MB-435S) were infected with AdCMVLuc preincubated with varying ratios of bsAb (expressed as the molar ratio of bsAb per fiber molecule). Experiments were performed either with (black bars) or without (white bars) the addition of soluble fiber knob to the cells prior to infection to assess the effect of CAR receptor blockade. Panels B and C, Luciferase expression and gene delivery were also assessed in various tissues *in vivo* following tail-vein injection of 10^{10} particles of

AdCMVLuc with (+) or without (-) bsAb. Values for individual mice are shown as circles, with means and standard deviations shown by horizontal and error bars. Significant differences between experimental and control groups are indicated by asterisks (*; $p<0.05$), daggers (†; $p\leq0.01$), and double daggers ($p\leq0.001$). Panel B, luciferase expression in relative light units (RLU) per mg tissue. Panel C, biodistribution of viral DNA measured by real time PCR, in copies per mg tissue. Panels D -F, Effect of docetaxel on bsAb retargeting of AdCMVLuc in tumor-bearing mice. 10^{10} particles of AdCMVLuc pre-incubated with either bsAb (+) or control (-) antibody to retarget receptor binding were injected into tumor-bearing mice pretreated with docetaxel. Panel D, bioluminescent imaging of luciferase expression in tumor bearing mice receiving docetaxel with 10^{10} particles of AdCMVLuc plus either control Ab or bsAb. Mice were imaged for 3 minutes and regions of interest used for quantifying luciferase expression are shown by red circles, with red indicating the highest level of signal intensity. Panel E, luciferase expression in relative light units (RLU) per mg tissue. Panel F, biodistribution of viral DNA in copies per mg of tissue.

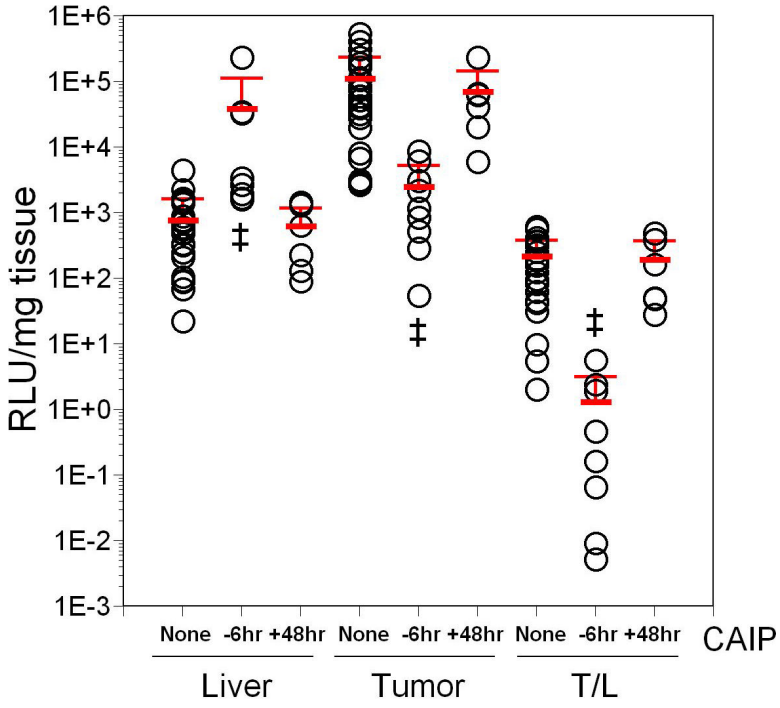

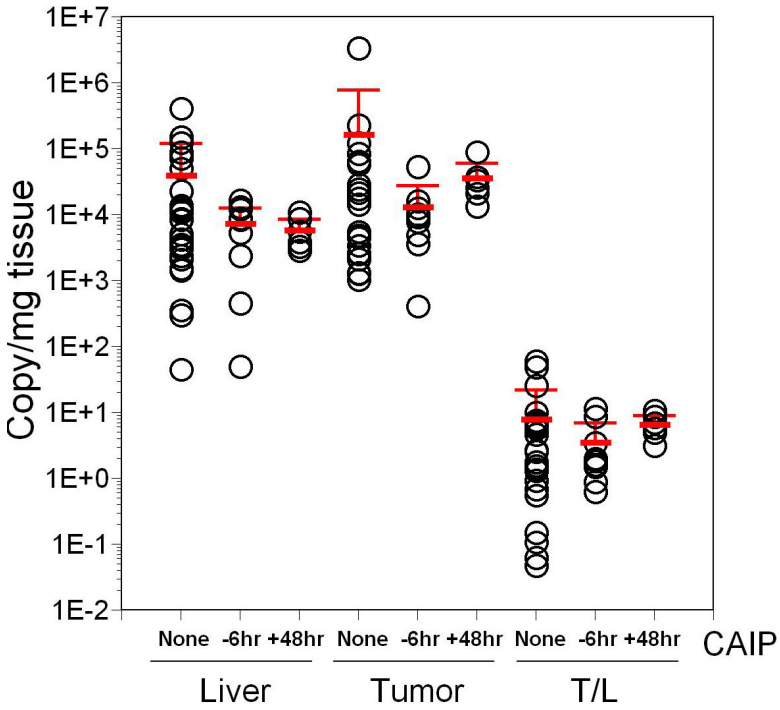

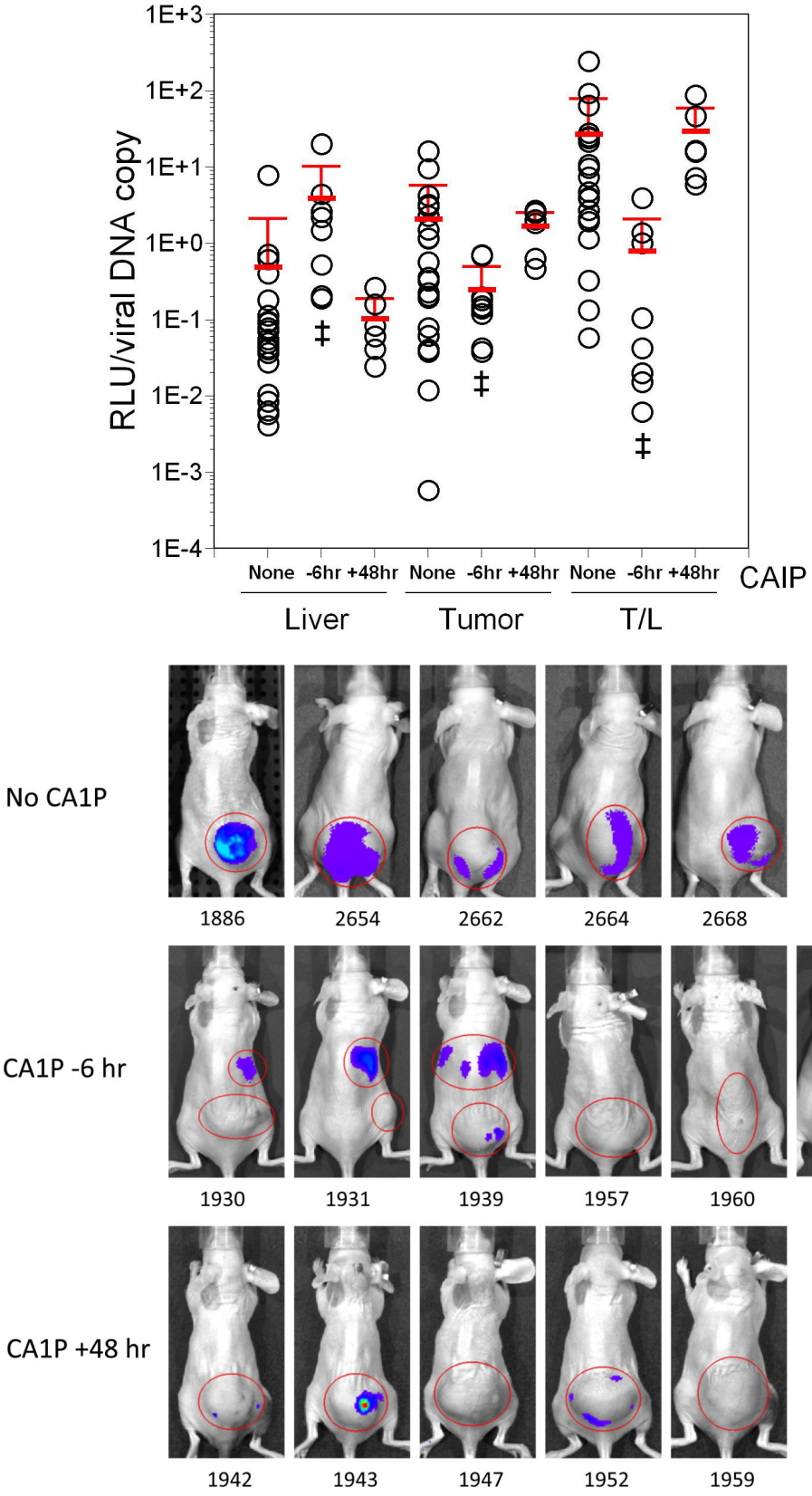

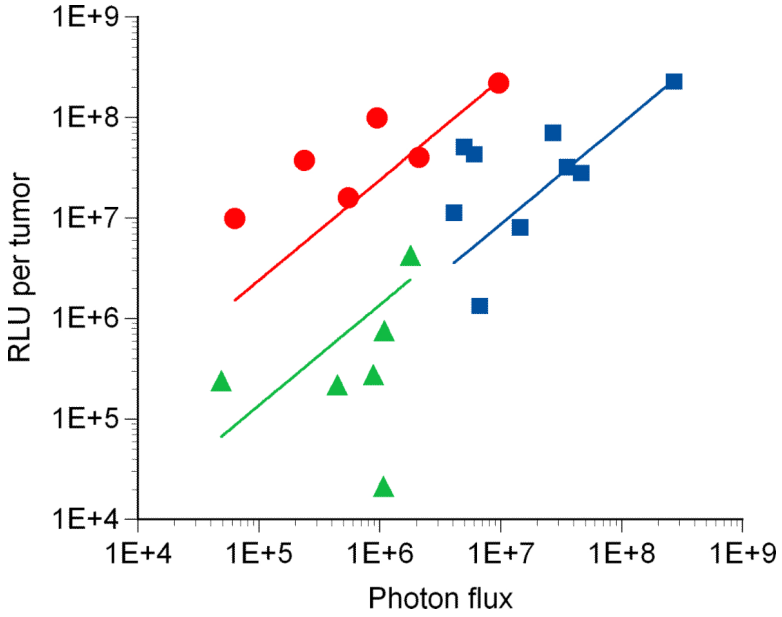

Figure 4. Effect of combretastatin A-1 phosphate (CAIP) on AdCMVLuc gene transfer and expression in tumor-bearing mice

10^{10} particles of AdCMVLuc were administered to mice pretreated with or without (none) CAIP injected either 6 hours before or 48 hours after the administration of vector. Values for individual mice are shown as circles, and mean and standard deviation are shown by horizontal and error bars. Significant differences between experimental and control groups are indicated by double daggers ($p \leq 0.001$). Panel A, luciferase expression per mg of tissue in the liver and tumor. Panel B, biodistribution of viral DNA, in copies per mg of tissue in tumor and liver. Panel C, Normalized luciferase expression measured by RLU per viral DNA copy. Panel D, bioluminescent imaging of luciferase expression in tumor bearing mice receiving 10^{10} particles of AdCMVLuc with or without CA1P. Mice were imaged for 1 minute and regions of interest used to quantify luciferase expression are outlined by red circles, with red indicating the highest level of signal intensity. Panel E, correlation of total tumor flux determined by bioluminescent imaging with biochemically determined luciferase activity (RLU/tumor). Squares, mice injected with 10^{10} particles of AdCMVLuc without CA1P; triangles, mice pre-injected with CA1P 6 hours prior to AdCMVLuc administration; circles, mice injected with CA1P 48 hours following AdCMVLuc administration.